

# **3 THE SUB-AUDIO MAGNETICS CONCEPT**

## **3.1 Introduction**

High spatial resolution in geophysical measurement can only be achieved economically when the instrumentation and field procedure permit rapid measurement and recording of the parameter of interest. Having reviewed the major galvanic-source geophysical exploration techniques, it was apparent that they all had inherent logistical constraints which would prevent their survey efficiency from ever approaching that achieved by High Definition Magnetism.

In the case of the electrical techniques, ER and EIP, the major constraint was the requirement for establishing grounded electrodes. MMR and MIP overcame this particular constraint by replacing electrodes with a horizontal component magnetometer. However, any advantage attained by circumventing the need for electrical contact with the ground was largely negated by the equally time consuming demand that the magnetometer sensors be precisely levelled and oriented. It was apparent that an innovative approach to electrical measurement was necessary if these parameters were to be measured with sufficient rapidity and efficiency to compare with that achieved in magnetic mapping.

The Sub-Audio Magnetic (SAM) method was developed as a solution to the problems of ER, EIP, MMR and MIP. However, it has the major additional performance advantage that multiple electrical parameters plus the spatially-varying magnetic field

are all mapped simultaneously. The SAM technique achieves this unique efficiency by using an optically-pumped, total field, magnetic resonance oscillator as both a magnetometer and an electromagnetic sensor.

In fact, the concept of using a total field magnetometer to monitor electromagnetic fields is itself, not new. A method using a proton precession magnetometer to determine electric current distribution was described by Breiner (1973). Suggested applications included measuring the effect of electric trains, high voltage power lines and the detection of buried pipe-lines or other man-made conductors. Also described was the application of a total field magnetometer to obtain a measure of subsurface conductivity as an aid to geological exploration. The method for doing this involved the introduction of direct current into the ground for a period which overlapped the measurement time of the magnetometer. These total field measurements were described by Breiner (*ibid.*, 55) as follows:

*"The current should be switched in polarity during consecutive readings at one location using the difference in readings as a measure of current density; the electrode array should be set up with consideration for the Earth's field direction and the magnetometer can be used as well for conventional field measurements when the current is removed".*

The method described was probably quite effective. However, the field practice was slow making the technique inefficient for high definition mapping. Breiner (*ibid.*) was aware that major advantages of this method were avoidance of the need for

- (i). sensor precise orientation and leveling of the sensor, and
- (ii). making ground contact with electrodes.

However, at the time, total field MMR surveys never gained popularity, most probably due to the fact that proton precession type magnetometers were intolerant of rapidly changing or alternating fields.

The SAM concept only became feasible as a result of improvements in magnetometer technology resulting from recent developments in digital electronics. Modern instruments are now capable of recording high precision, total magnetic field measurements at kilohertz sample rates.

## 3.2 Sub-Audio Magnetics

Sub-Audio Magnetics is described in an International Patent by Cattach *et al.* (1991) and in a subsequent concept paper by Cattach *et al.* (1993). A more recent description of the technique was given by Cattach *et al.* (1995a). The SAM method requires a time-varying electric current to be artificially applied to the ground. This is achieved with a high power transmitter producing a broadband (low frequency square wave) signal that is introduced into the ground either through distant electrodes as for conventional gradient array ER or MMR surveys, or induced into the ground through a loop as for conventional electromagnetic surveys. In either case, the electromagnetic signal from the time-varying current induced in the ground is then measured simultaneously with the Earth's spatially-varying magnetic field using a total field, rapid sampling magnetometer.

The combined signals are sampled at a fast enough rate to adequately measure the full spectrum of the artificial waveform. The signals from the two magnetic sources are spectrally distinct and with the aid of digital signal processing techniques, they may be separated and processed in real-time. The benefit of having this ability is the efficient, concurrent, high definition mapping of parameters related to the electrical characteristics of the ground as well as the spatially-varying magnetic field.

### 3.2.1 Survey Speed

The Sampling Theorem states that in order to adequately sample a waveform, at least two samples per shortest wavelength are required to define all frequency components (Blackman and Tukey, 1958; Bracewell, 1978). Empirical experiments on a magnetic noise spectrum by Sertsrivanit (1986) demonstrated that more than 99% of the energy was contained in wavelengths longer than twice the depth to the top of the source. Consequently, assuming the nearest source to be at ground level, the shortest significant wavelength in a magnetic profile will be equal to twice the sensor elevation. That is,

$$\lambda_{Max(Spatial)} = \frac{1}{2h} \quad \text{Eqn 3-1}$$

where  $f_{Max(Spatial)}$  = the highest frequency of spatial origin  
 $h$  = the height of the sensor above ground

To meet the requirements of the Sampling Theorem, magnetic measurements must, therefore, be taken at intervals of no greater than the elevation of the sensor above ground. Sampling at greater intervals will result in aliased waveforms that are invalid for filtering or proper interpretation (Stanley *et al.*, 1992).

If we consider that the magnetic sensor is operated at a height  $h$  above the ground surface and moved at a maximum velocity  $V$ , then the highest spatial frequency in the magnetic profile translates to a maximum time-varying frequency ( $f_{Max(Time)}$ ) given approximately by the relationship:

$$f_{Max(Time)} = \frac{V}{2h} \quad \text{Eqn 3-2}$$

For example, the rate at which the spatially-varying magnetic field changes for a magnetic sensor traversing at 2.0 m/s (7.2 km/h) at an elevation of 1 m above ground, will have a 40 dB cutoff at about 1 Hz. Clearly, in order to be able to separate the applied signal from the spatially-varying magnetic field, the transmitter frequency must be greater than  $f_{Max(Time)}$ . Naturally occurring temporal changes in the magnetic field may be removed by reference to a synchronised stationary magnetic sensor as for conventional magnetic surveying.

### 3.2.2 TFMMR / TFMMIP

SAM may prove to have a wide range of applications including mapping, profiling and downhole logging. As an initial priority, the feasibility studies targeted its role as a high definition electrical mapping tool which would complement high definition magnetics. In this mode, the survey configuration closely parallels Magnetometric Resistivity (MMR) and Magnetic Induced Polarisation (MIP) both of which are described in the previous chapter.

The fundamental difference between these SAM surveys and conventional MMR / MIP is that the Total Magnetic Intensity is measured instead of a horizontal component. Consequently, in order to distinguish the information recorded from MMR and MIP, the

terms “Total Field Magnetometric Resistivity” (TFMMR) and “Total Field Magnetometric<sup>1</sup> Induced Polarisation” (TFMMIP) have been adopted. A typical survey layout for a TFMMR / TFMMIP survey is shown in Figure 3-1.

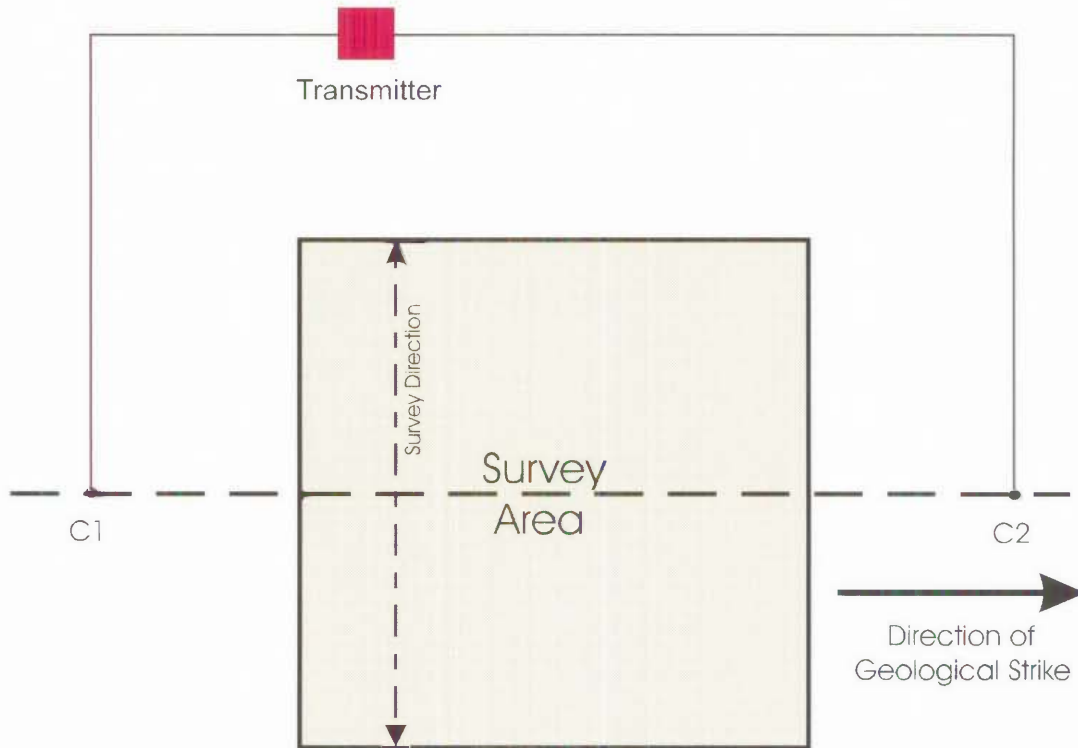


Figure 3-1. Layout of a typical TFMMR / TFMMIP survey showing the ideal electrode positions and survey orientation relative to the direction of geological strike. Current electrode positions are C<sub>1</sub> and C<sub>2</sub>.

### 3.3 Components of the SAM Signal

The total magnetic field intensity ( $H_T$ ) measured by an optically-pumped (total field) sensor is comprised of two major spectrally distinct components:

- The Spatially-varying magnetic field ( $H_S$ ) which will have a maximum frequency component as defined previously.
- The low frequency Modulation ( $H_{Mod}$ ) due to the transmitted signal.

<sup>1</sup> The term “magnetometric” was adopted for use here instead of “magnetic” as it was believed to more correctly indicate the *measurement* of magnetic fields as opposed to the implication that current flow is magnetically-induced. The term “Magnetic Induced Polarisation” was considered ambiguous for this reason.

The total magnetic field intensity is then:

$$H'_T = H_S + H_{Mod} \quad \text{Eqn 3-3}$$

$H_S$  and  $H_{Mod}$  may be separated by an appropriate filter.

Furthermore, the modulation ( $H_{Mod}$ ) will consist of:

- The *Primary* field ( $H_{Primary}$ ) which is due to current flow in the wires supplying the electrodes.
- The *Ground* field ( $H_G$ ) which is defined as the magnetic field due to current flowing through the ground.

The Normalised TFMMR ( $H_N$ ) anomaly will then be defined by:

$$H_N = H_{Mod} - H_{Primary} - H_{Normal} \quad \text{Eqn 3-4}$$

where  $H_{Normal}$  is the *Normal* magnetic field and is defined as the theoretical magnetic field measured by a total field magnetometer (i.e. in the direction of the Earth's magnetic field) over a homogeneous earth due to galvanically-induced current flow.

### 3.3.1 Calculation of the Primary Field

The magnetic field  $H$  due to electric current flowing in a long straight wire is directly proportional to the current  $I$  in the wire and inversely proportional to the distance  $r$  from the wire. That is:

$$H \propto \frac{I}{r} \quad \text{Eqn 3-5}$$

According to Ampere's law, a current  $\mathbf{I}$  flowing in any path can be considered as many infinitesimal current elements, such as that in Figure 3-2. If  $\Delta l$  represents any infinitesimal length along which the current is flowing, then the magnetic field  $\Delta \mathbf{H}$  at any point  $P$  in space, due to this element of current is given by Telford *et al.* (1990) as:

$$\Delta \mathbf{H} = (\mathbf{I} \Delta l) \times \frac{\mathbf{r}_1}{4\pi r^2} \quad \text{Eqn 3-6}$$

where  $r$  = the distance from the element  $\Delta l$  to the point  $P$ , and  
 $\mathbf{r}_1$  = the unit vector in the direction of  $r$ .

The magnitude of  $\Delta \mathbf{H}$  is:

$$\Delta H = \frac{I \Delta l \sin \theta}{4\pi r^2} \quad \text{Eqn 3-7}$$

The magnetic field due to the current flowing through the cable supplying the electrodes can, therefore, be calculated at any point in the survey area by integrating along the length of the cable. In the absence of significant topographic relief, the Primary field in the survey area can be assumed to be vertical at all measurement points.

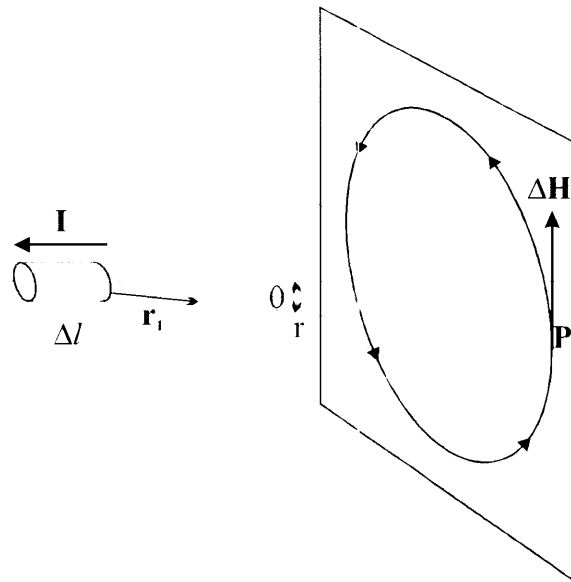


Figure 3-2. Ampere's Law - A current  $I$  passing through a length of conductor  $\Delta l$  creates a magnetising field  $\Delta \mathbf{H}$  at a point  $P$  (Drawn from Telford *et al.*, 1960).

### 3.3.2 Calculation of the Normal Field

The magnetic field at the surface caused by current flowing into grounded electrodes is described by Keller and Frischknecht (1966), Edwards (1974), Edwards and Nabighian (1991). The Normal magnetic field is the same as the field which would be produced by the same current flowing in a wire extending vertically downward from the earth's

surface to infinity. The components of the magnetic field at a point  $P_{(x,y)}$  for a single electrode located at (0,0) can again be calculated from Ampere's law with the result:

$$\begin{aligned} H_x &= \frac{I_y}{4\pi(x^2 + y^2)} \\ H_y &= \frac{I_x}{4\pi(x^2 + y^2)} \\ H_z &= 0 \end{aligned} \quad \text{Eqn 3-8}$$

Consequently, the Normal field has only horizontal components and can be calculated for two electrodes by vector addition.

### 3.4 Determination of Total Field Corrections

Because a total field magnetometer is being used, only the component of the artificially-induced magnetic field, in the direction of the Earth's magnetic field, is measured. Consequently, to make corrections for both the Primary and Normal magnetic fields, their components in the direction of the Earth's magnetic field must be calculated. In order to map the components of the Primary and Normal fields onto the direction of the Earth's magnetic field, it is first necessary to define in local grid coordinates, the unit vector representing the direction of the Earth's magnetic field.

In Figure 3-3,  $\mathbf{F}_E$  is a unit vector representing the direction of the Earth's magnetic field. The  $x$ ,  $y$  and  $z$  axes define the local grid coordinate system.  $I$  is the inclination of the Earth's magnetic field and the declination,  $D$  is the angle between  $\mathbf{F}_E$  and grid north. It can be shown that

$$\mathbf{F}_E = X_E \mathbf{i} + Y_E \mathbf{j} + Z_E \mathbf{k} \quad \text{Eqn 3-9}$$

where

$$\begin{aligned} X_E &= \cos D \cos I \\ Y_E &= \sin D \cos I \\ Z_E &= \sin I \end{aligned}$$

and  $\mathbf{i}$ ,  $\mathbf{j}$  and  $\mathbf{k}$  are unit vectors in the  $x$ ,  $y$  and  $z$  directions, respectively.



The amplitude of the applied magnetic field in the survey area is insignificant compared to the magnitude of the Earth's magnetic field. Consequently, the vector addition of the applied field to the Earth's magnetic field will have little effect on its direction. The influence that the applied field will have on total field measurements can, therefore, be approximated by projecting the applied field onto the direction of the Earth's magnetic field. This can be performed by calculating the scalar product of the applied field with the unit vector defining the direction of the Earth's magnetic field.

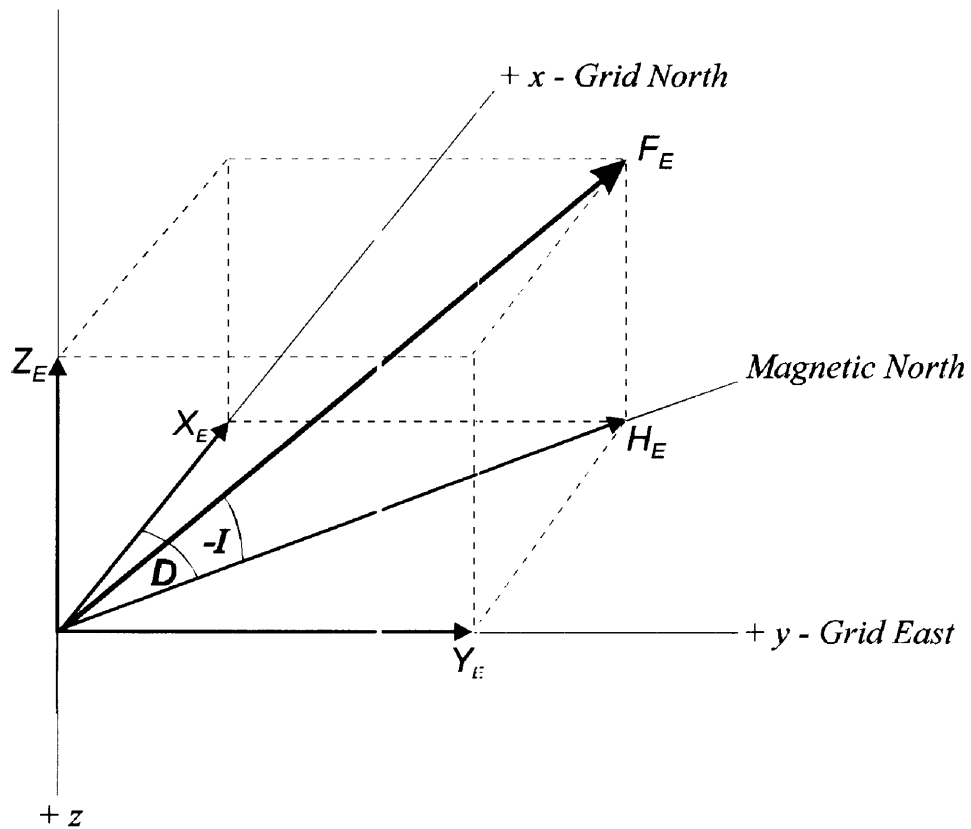


Figure 3-3. Elements of the Earth's magnetic field with respect to a local coordinate system.

With respect to Figure 3-4, let  $\mathbf{F}_A$  be an applied magnetic field defined as follows:

$$\mathbf{F}_A = X_A \mathbf{i} + Y_A \mathbf{j} + Z_A \mathbf{k} \quad \text{Eqn 3-10}$$

Then

$$\mathbf{F}_A \cdot \mathbf{F}_E = |\mathbf{F}_A| |\mathbf{F}_E| \cos \theta \quad \text{Eqn 3-11}$$

where  $\mathbf{F}_A$  is the applied field, and  $\mathbf{F}_E$  is the unit vector in the direction of the Earth's magnetic field. Since  $|\mathbf{F}_A|\cos\theta$  is the projection of  $\mathbf{F}_A$  on  $\mathbf{F}_E$ , then

$$\mathbf{F}_A \cdot \mathbf{F}_E = |\mathbf{F}_E| \times (\text{projection of } \mathbf{F}_A \text{ on } \mathbf{F}_E) \quad \text{Eqn 3-12}$$

It can also be shown that

$$\mathbf{F}_A \cdot \mathbf{F}_E = X_A X_E + Y_A Y_E + Z_A Z_E. \quad \text{Eqn 3-13}$$

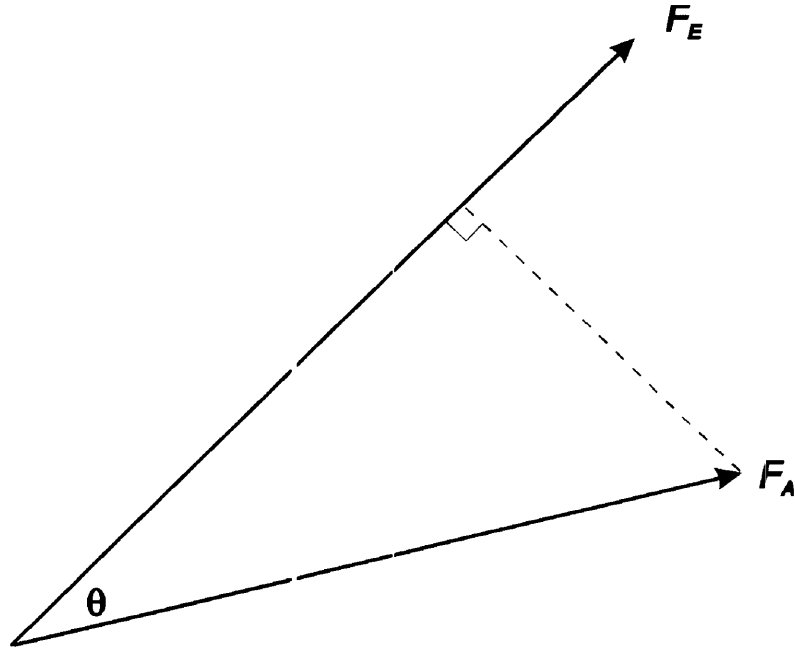


Figure 3-4. Projection of an applied field  $\mathbf{F}_A$  onto a unit vector defining the direction of the Earth's magnetic field  $\mathbf{F}_E$ .

Because, the Primary field has only a vertical component, its influence on total field measurements is affected by the inclination  $I$  of the Earth's magnetic field. The Primary field for a typical TFMNR / TFMIP array is shown in Figure 3-5. The Inclination and Declination used to generate the image were  $60^\circ$  and  $25^\circ$ , respectively.

The corresponding Normal magnetic field expected over a homogeneous earth is shown in Figure 3-6. Because the Normal field has only horizontal components, its shape is influenced greatly by the declination  $D$ . The Normal field is asymmetric for all declinations other than  $0^\circ$ .

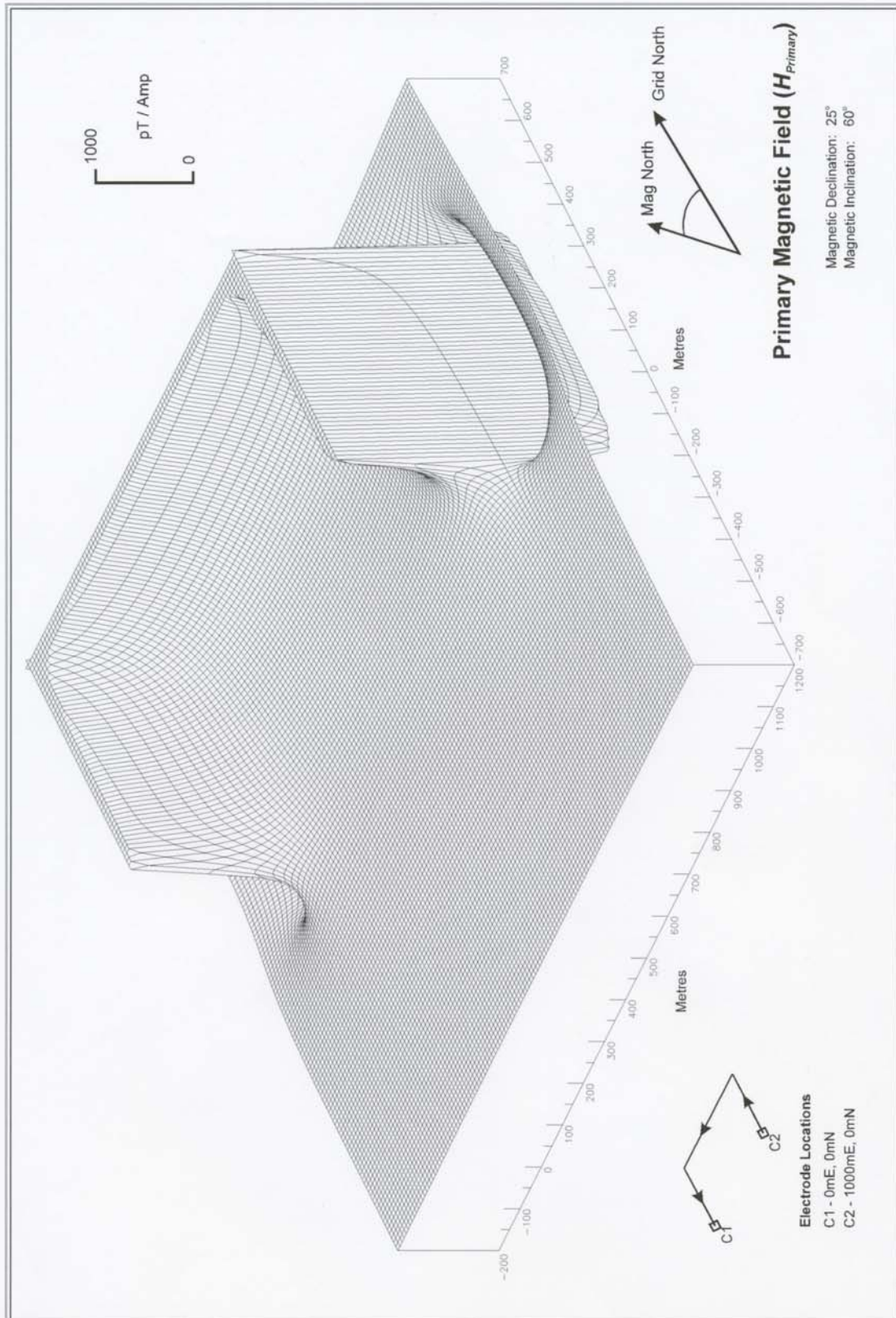


Figure 3-5. The theoretical Primary field ( $H_{Primary}$ ) as measured with a total field magnetometer, resulting from current flowing through cables feeding grounded electrodes at positions C1 and C2.

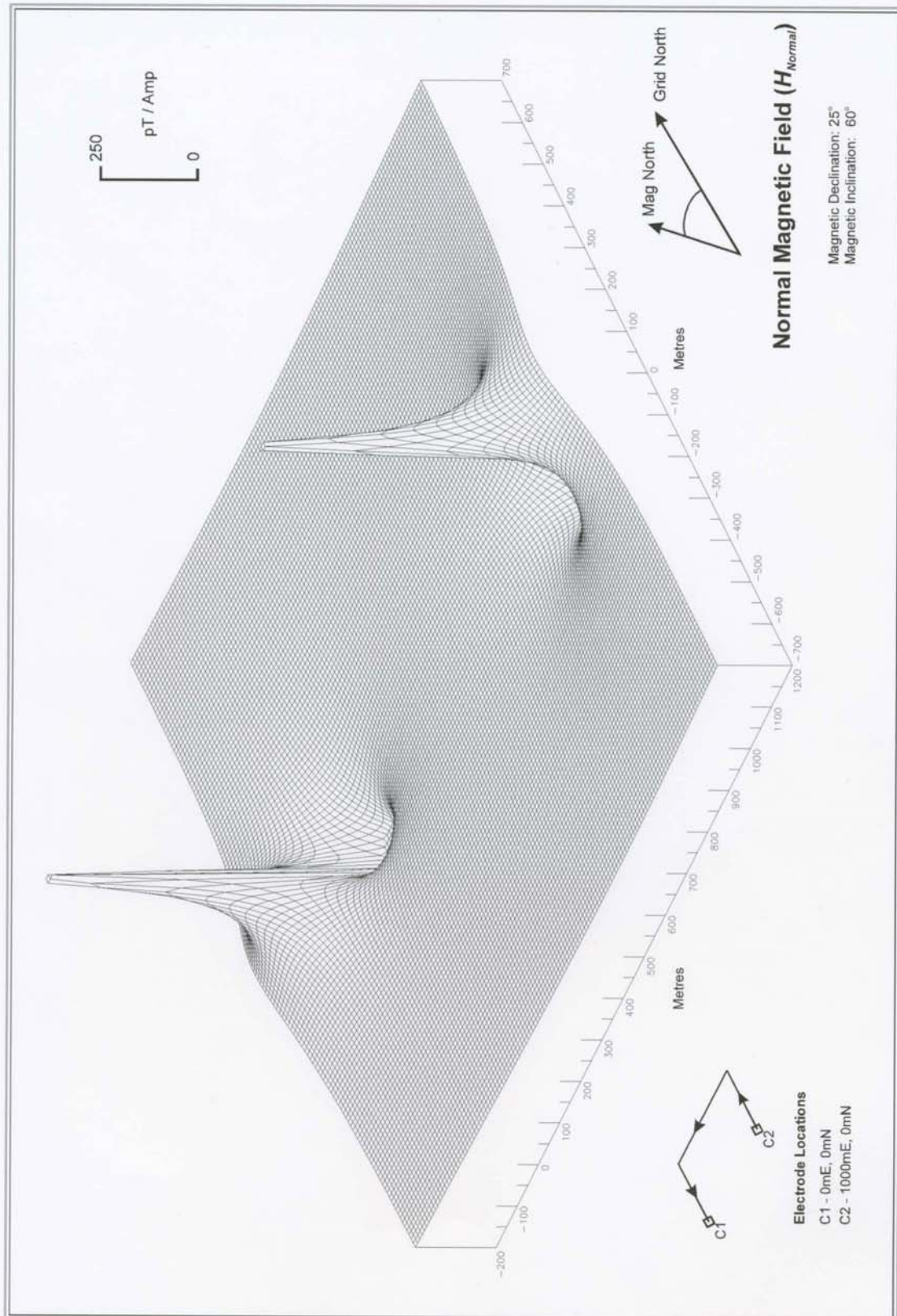


Figure 3-6. The theoretical Normal field ( $H_{Normal}$ ) as measured with a total field magnetometer due to current flowing through a homogeneous earth.



### 3.5 Analytical Solutions for Total Field Magnetometric Resistivity (TFMMR)

The analytical solutions for magnetostatic fields resulting from galvanic current flow are described for simple geometries by Edwards *et al.* (1978) and by Edwards and Nabighian (1991). Generally, they are described for one or two components, usually the vertical and/or the horizontal component perpendicular to the line joining the electrodes. The theoretical TFMMR anomalies expected over simple model structures are described by Fathianpour and Cattach (1995). In that paper, responses are illustrated for an homogeneous isotropic and anisotropic earth, vertical contacts and faults, thick dykes and outcropping hemispherical depression models. For each model, comparisons are made between the theoretical TFMMR response and the theoretical response calculated for the MMR method.

As an example, Figure 3-7 shows the geometry used to define a vertical fault model separating two media with different resistivities  $\rho_1$  and  $\rho_2$  where  $\rho_2 = 3\rho_1$ . With the current point electrode situated on the fault line at the point ( $x=0$ ;  $z=0$ ) the X (MMR component), Y and Z anomalous magnetic field components were calculated for a profile traversing the structure in the X-direction and located 500 m distant from the electrode. The results are shown for a current flow of one Amp together with the corresponding TFMMR anomaly in Figure 3-8.

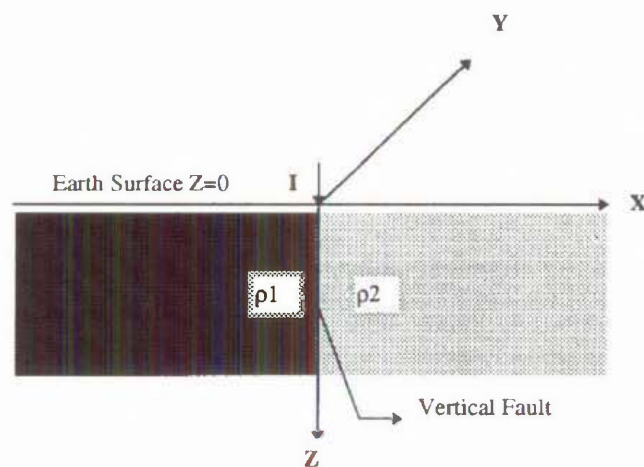


Figure 3-7. Geometry used to define a vertical fault model separating two media with different resistivities (After Fathianpour and Cattach, 1995).

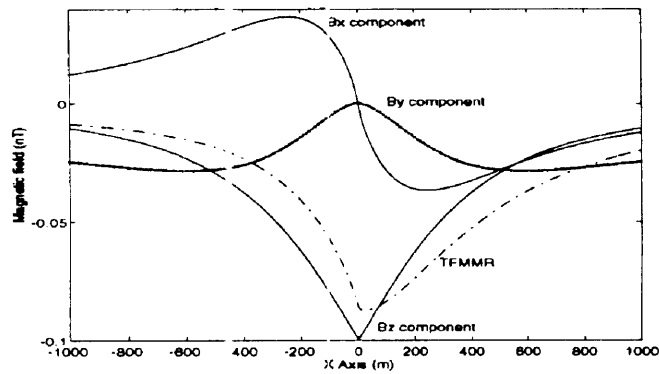


Figure 3-8. Horizontal X, Y and vertical Z components of the anomalous magnetic field for the vertical fault model. Notice the relative magnitude of the -Z component compared to those of the horizontal component (After Fathianpour and Cattach, 1995).

As with total field magnetic anomalies, the shapes of TFMMR anomalies are influenced by the inclination and declination of the Earth's magnetic field. Figure 3-9 shows the effect of varying the inclination of the geomagnetic field on the shape of the TFMMR anomaly from Figure 3-8 for a fixed declination of  $25^\circ$ . Similarly, the result of varying the declination with a fixed inclination of  $60^\circ$  is illustrated in Figure 3-10. In areas of low latitude, the shape of the TFMMR anomaly will be determined largely by the horizontal components. Conversely, at high latitudes, the vertical component will be dominant.

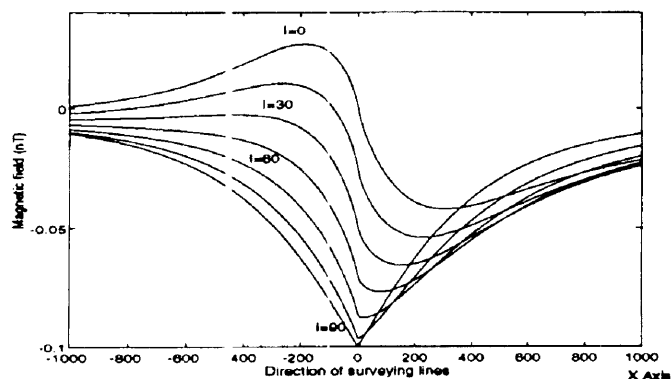


Figure 3-9. Profiles showing the influence of the geomagnetic field inclination on TFMMR measurements for a fixed declination of  $25^\circ$  (After Fathianpour and Cattach, 1995).

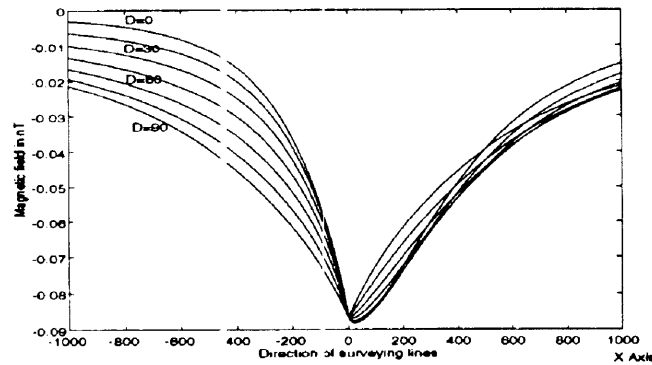


Figure 3-10. Profiles showing the influence of the geomagnetic field declination on TFMMR measurements for a fixed inclination of  $60^\circ$  (After Fathianpour and Cattach, 1995).

The comparisons of the TFMMR and MMR anomalies described by Fathianpour and Cattach (*ibid.*) for simple models demonstrate that both methods are sensitive to the basic geometry of the models and conductivity contrasts. However, the TFMMR signal is governed by the combined effect of the three components as well as the attitude of the Earth's magnetic field. For 2-dimensional structures such as faults and dykes, the magnitude of the theoretical responses for TFMMR and MMR are similar. In situations where conductive bodies strike perpendicular to the direction of current flow, the MMR signal is quite small whereas the TFMMR response is theoretically still measurable.

## 3.6 Factors Affecting Data Quality

### 3.6.1 The Earth's Ambient Electromagnetic Field

Electrical geophysical surveys must be conducted in the presence of the Earth's ambient electromagnetic field. There are numerous sources of the electromagnetic field which include industrial, atmospheric, oceanic, electrochemical, acoustic and extraterrestrial. The noise spectrum will vary substantially at different locations and at different times of the day and year. The electromagnetic environment of the Earth is described by Keller and Frischknecht (1966) and Zhdanov and Keller (1994). An excellent review of the subject is also given by Macnae *et al.* (1984). The components of the electromagnetic noise spectrum are shown in Figure 3-11.

All of the above noise sources have some effect on conventional magnetic surveys although the interference is generally quite small compared with the intensity of the Earth's steady magnetic field. The degree of interference will, of course, depend on the amplitude and frequency of the phenomena. However, the signals expected from a SAM survey are quite small ( $< 20 \text{ nT}$ ) and it was anticipated at the outset of the project that electromagnetic noise in the frequencies of interest may be a limiting factor to the application of the technique. Consequently, an awareness of the relevant noise sources was essential in order to enable the development of appropriate noise suppression strategies.

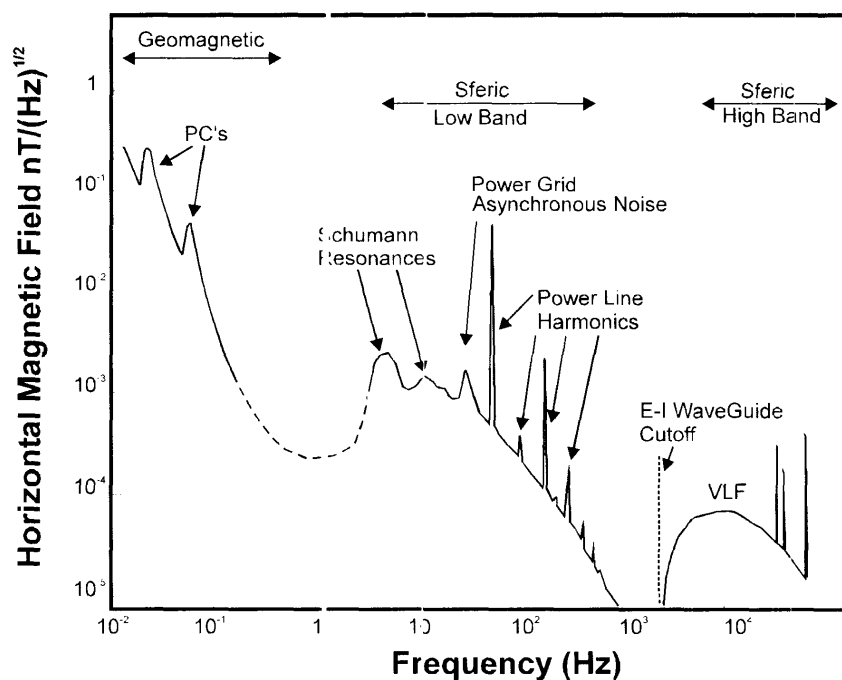


Figure 3-11. Components of the electromagnetic noise spectrum (After Macnae *et al.*, 1984).

The sources of electromagnetic noise considered most relevant to the SAM technique include the following:

- (i). **Diurnal variation.** Phenomena with a periodicity of about one day due to the interaction of the solar wind with the Earth's magnetic field.
- (ii). **Magnetic storms.** Periods of rapid, irregular, transient fluctuations of the magnetic field which occur during sunspot activity. They are of greater amplitude (50-200 nT), more irregular and of higher frequency than diurnal variation.



- (iii). **Micropulsations.** Small amplitude fluctuations in the Earth's magnetic field due to small scale disturbances in the external magnetic field. They are described as quasi-periodic with frequencies in the range of millihertz (mHz) to a few Hz with amplitudes typically of less than a nanotesla.
- (iv). **Sferics.** Natural transients generated by lightning discharges. They occur in the natural noise spectrum in the 5 Hz - 25 kHz range (Macnae *et al.*, 1984). Propagation of a sferic to the survey site may be either direct, if the lightning is nearby or by multiple reflection off the Earth-ionosphere waveguide if the lightning is distant from the site.
- (v). **Schumann resonances.** These occur when the ELF components of sferics travel completely around the Earth and interfere either constructively or destructively. Low order mode frequencies occur at 8, 14, 20 and 26 Hz (Sheriff, 1991).
- (vi). **Industrial noise.** This is due to 50/60 Hz electromagnetic noise due to industrial electrical power. The frequency is generally closely controlled although as demand on a power distribution network increases, surges occur which can introduce transient shifts in frequency (commonly 1-2 Hz). Some distortion of the ideal sinusoidal waveform is always present which results in harmonic components of the mains power frequency. The odd harmonics are generally orders of magnitude greater than the even harmonics.

In terms of conducting SAM surveys, the above sources of electromagnetic noise will have the following ramifications:

- Assuming that the transmitter frequency is higher than the highest significant geomagnetic field variation, that variation will be effectively removed from the SAM signal by the high pass filter. The spatially-varying magnetic field will be corrected for geomagnetic field variation as per conventional magnetic surveys with the aid of a base station magnetometer.
- Electromagnetic noise in the frequency band of interest such as the Schumann resonances and micropulsations, will be a source of noise in the SAM data. However, the amplitude of the noise is expected to be small ( $\approx 0.01$  nT) which is likely to be within the noise level inherent in the instrumentation.

- Industrial noise can be a serious problem when surveying in areas proximal to power lines. A facility is required to filter the mains power frequencies and their significant harmonics

Higher frequency noise (say, above 500 Hz) will not be adequately sampled by the system due to sample rate limitations and if the amplitudes are significant, will require the use of an anti-aliasing filter.

### 3.6.2 Electromagnetic Induction (EM Coupling)

When an alternating current flows through either a loop of wire or through a wire grounded at both ends, a time-varying magnetic field is generated. As has been discussed earlier, that field is generally called the *Primary* field ( $H_{Primary}$ ) due to the source current. If a conductor is present within the alternating magnetic field, *induced* or *eddy* currents are generated within the conductor. These currents subsequently generate their own *Secondary* magnetic fields. It is the detection and analysis of the Secondary magnetic fields due to eddy currents induced in conductors which is the basis of all *induction* methods, commonly referred to as *electromagnetic* methods.

Nabighian (1991, 3) describes MMR as “*essentially a DC technique*” although in practice, time-varying currents are used. The models proposed for the technique generally neglect the effect of the secondary magnetic fields resulting from electromagnetic induction since:

*“It is assumed that the frequencies selected (1 - 5 Hz) are sufficiently low that the amplitudes of the induced currents are negligible in comparison with the amplitudes of the galvanic currents”* (Edwards, 1974, 1137).

However, as would be expected due to the relatively small amplitude of the IP signal, MIP parameters appear to be more susceptible to the influence of electromagnetic coupling (Hishida *et al.*, 1993).

As described by Telford *et al.* (1990), EM coupling may be reduced in time domain IP surveys by using the later (low frequency) portion of the decay curve to determine chargeability values. The same improvement may be obtained with frequency domain systems by using only low frequencies (say less than 3 Hz).